

dynamical data is available from chemical shift spectra of oriented samples. And fourthly, the determination in situ of the  $^{14}\text{N}$  electric field gradient tensor opens up the possibility of using this nucleus for high resolution studies as pioneered by Opella and co-workers.<sup>24</sup>

**Acknowledgment.** The authors thank Prof. Dan Urry for the gift of cyclo[ $^{13}\text{C}_1$  Val-Gly-Pro-Val-Gly] peptide synthesized with support from the National Institutes of Health Grant No. HL-29578. The FSU Computing Center is gratefully acknowledged

for considerable computing time. We are deeply indebted to Richard Rosanske and Thomas Gedris for their skillful maintenance, modification, and repair of the NMR spectrometers. This work was supported by the National Science Foundation Grant Nos. DMB-9005938 and DMB-8451876 with Procter and Gamble through a Presidential Young Investigator Award to T.A.C. as well as an Alfred P. Sloan Fellowship to T.A.C.

Registry No. Gramicidin A, 11029-61-1.

## Ultraviolet Resonance Raman Study on the Binding Mode of Enkephalin to Phospholipid Membranes

Hideo Takeuchi, Yoshikazu Ohtsuka, and Issei Harada\*

Contribution from the Pharmaceutical Institute, Tohoku University, Aobayama, Sendai 980, Japan. Received October 29, 1991

**Abstract:** Ultraviolet Resonance Raman spectra have been measured of Met-enkephalin (Tyr-Gly-Gly-Phe-Met) and Leu-enkephalin (Tyr-Gly-Gly-Phe-Leu) incorporated into phospholipid liposomes. The 213-nm Raman spectra in the amide I and III regions have shown that these opioid peptides take a folded conformation in the lipid-bound state. The environments of aromatic side chains of Tyr<sup>1</sup> and Phe<sup>4</sup> are monitored by the 240-nm Raman scattering intensities of the side chain vibrations. Tyr Raman bands generally gain intensity on going from aqueous solution to the liposome-bound state, indicating that the phenolic ring of Tyr is buried in the hydrophobic region of the lipid bilayer. On the other hand, Phe does not show intensity change, suggesting that the Phe side chain is exposed to the aqueous phase or located in the hydrophilic region of the bilayer. The insertion of the Tyr side chain into the membrane is deeper for Met-enkephalin than for Leu-enkephalin. Paralleling experiments on [Trp<sup>4</sup>]Met-enkephalin (Tyr-Gly-Gly-Trp-Met) have shown that this peptide also takes a folded conformation in liposomes with the Tyr side chain inserted into the membrane hydrophobic interior. The Trp side chain is located in the hydrophilic region as in the case of Phe side chain of natural enkephalins. The degree of insertion of the Tyr side chain into membrane bilayers correlates with the receptor affinity and opiate activity of the peptide.

### Introduction

The primary structure of enkephalin is Tyr-Gly-Gly-Phe-X, where X is Met (Met-enkephalin) or Leu (Leu-enkephalin). These endogenous peptides bind preferentially to  $\delta$ -opioid receptors embedded in cell membranes and elicit morphine-like analgesic response.<sup>1</sup> The conformation of enkephalin has been studied extensively by using various experimental and theoretical methods, particularly in connection with the structure-activity relationships.<sup>2</sup> However, the active conformation of enkephalin in the receptor site has not been established yet. The difficulties in determining the active conformation mainly arise from the following reasons. First, the opioid receptors, which are membrane proteins, have not been isolated to such a high purity that spectroscopic or crystallographic studies can be made on their complexes with agonists. Second, enkephalin contains two Gly residues that make the pentapeptide highly flexible. The flexibility is exemplified by the conformational variety observed in solution and in the crystalline state.<sup>2</sup> Hence, the various conformers found in solutions and crystals or predicted by conformational energy calculations cannot be related immediately to the active conformer.

A catalytic role of cell membranes in the opiate-receptor binding process has been postulated to account for large apparent association constants between the opioid peptides and receptors.<sup>3-5</sup>

According to the hypothesis, the polar lipid surface of the cell membrane attracts the amphiphilic opioid peptide, hydrophobic interaction facilitates the entry of the peptide into the membrane with concomitant conformational change to a specific structure suitable for binding to the receptor, and then the peptide binds to the receptor as a result of migration within the membrane. This proposed mechanism was employed to explain the correlation between the receptor subtype specificities of opioid peptides and their affinities to phospholipids.<sup>6,7</sup> A similar mechanism has been proposed for the binding of hormone peptides to their membrane-bound receptors.<sup>8,9</sup> In this connection, the interaction of enkephalin with lipid micelles or liposomes has been studied by NMR<sup>3,10-14</sup> and FT-IR<sup>15</sup> spectroscopy. The previous studies concluded that enkephalin takes a folded structure in membrane environments in contrast to an equilibrium of several unfolded conformers in aqueous solution. Currently, the mode of binding to membranes is argued in relation to the opiate activity.<sup>14</sup>

Ultraviolet resonance Raman (UVRR) spectroscopy is a useful tool to investigate the structures of peptides bound to lipid membranes because the Raman scattering from lipids is negligibly weak with UV excitation compared to the resonance-enhanced

(1) Hughes, J.; Smith, T. W.; Kosterlitz, H. W.; Fothergill, J. A.; Morgan, B.; Morris, H. R. *Nature* 1975, 258, 577.

(2) For a review, see: Schiller, P. W. In *The Peptides*; Udenfriend, S., Meienhofer, J., Eds.; Academic Press: Orlando, FL, 1984; Vol. 6, pp 219-268.

(3) Deber, C. M.; Behnam, B. A. *Proc. Natl. Acad. Sci. U.S.A.* 1984, 81, 61.

(4) Deber, C. M.; Behnam, B. A. *Biopolymers* 1985, 24, 105.

(5) Sargent, D. F.; Schwyzer, R. *Proc. Natl. Acad. Sci. U.S.A.* 1986, 83, 5774.

(6) Gysin, B.; Schwyzer, R. *Arch. Biochem. Biophys.* 1983, 225, 467.

(7) Schwyzer, R. *Biochemistry* 1986, 25, 6335.

(8) Wakamatsu, K.; Okada, A.; Miyazawa, T.; Masui, Y.; Sakakibara, S.; Higashijima, T. *Eur. J. Biochem.* 1987, 163, 331.

(9) Schwyzer, R. *EMBO J.* 1987, 6, 2255.

(10) Jarrell, H. C.; Deslauriers, R.; McGregor, W. H.; Smith, I. C. P. *Biochemistry* 1980, 19, 385.

(11) Zetta, L.; Hore, P. J.; Kaptein, R. *Eur. J. Biochem.* 1983, 134, 371.

(12) Behnam, B. A.; Deber, C. M. *J. Biol. Chem.* 1984, 259, 14935.

(13) Zetta, L.; De Marco, A.; Zannoni, G. *Biopolymers* 1986, 25, 2315.

(14) Milon, A.; Miyazawa, T.; Higashijima, T. *Biochemistry* 1990, 29, 65.

(15) Surewicz, W. K.; Mantsch, H. H. *Biochim. Biophys. Res. Commun.* 1988, 150, 245.

Raman scattering from the main chain and aromatic side chains of peptides. The structural information obtainable from UVRR spectra includes microenvironments, hydrogen bonding states, and conformations of aromatic side chains as well as the peptide main chain structure. Particularly, the capability of obtaining information on microenvironments of aromatic side chains is one of the characteristics of UVRR spectroscopy. Even a small change in the resonant electronic transition caused by an environmental change may be sensitively reflected in the UVRR scattering intensity.<sup>16-19</sup> In this work, we have measured UVRR spectra of Leu- and Met-enkephalins incorporated into phospholipid liposomes and compared the spectra with those recorded in aqueous solution. The comparison has shown that both enkephalins take a folded main chain conformation when bound to lipid membranes, and the Tyr side chain is buried in the hydrophobic interior of the membrane but the Phe side chain is not. The present finding on the environments of the Tyr and Phe side chains is not consistent with the lipid-binding model proposed by a recent NMR study utilizing the transferred nuclear Overhauser effect (TRNOE).<sup>14</sup>

### Experimental Section

Met- and Leu-enkephalins were purchased from Sigma in the acetate salt form and used without further purification. [Trp<sup>4</sup>]Met-enkephalin was synthesized on a solid-phase peptide synthesizer (Pharmacia, Biolyx 4175) using the 9-fluorenylmethoxycarbonyl (Fmoc) method. The resin and Fmoc amino acids were purchased from MilliGen/Bioscience. The crude peptide was purified on a Jasco 880 HPLC with a reversed-phase column (Nacalai SC18-AR, 1.0 × 25 cm). Elution was performed isocratically with 0.1% trifluoroacetic acid–20% acetonitrile in H<sub>2</sub>O at a flow rate of 3 mL/min and monitored at 278 nm. The purified peptide was identified by <sup>1</sup>H NMR (Jeol JNM-GX500). Dilauroyl-L- $\alpha$ -phosphatidylcholine (DLPC) and dipalmitoyl-DL- $\alpha$ -phosphatidyl-L-serine (DPPS) were obtained from Sigma and used without further purification. Amino acid derivatives, *N*-acetyl-L-tyrosine ethyl ester (AcTyrEE) monohydrate and *N*-acetyl-L-phenylalanine ethyl ester (AcPheEE), were purchased from Aldrich and Sigma, respectively.

Aqueous solution of enkephalin was prepared at a concentration of 3 mM (Met- and Leu-enkephalin) or 1 mM ([Trp<sup>4</sup>]Met-enkephalin). No buffer was added to the solution to minimize the ionic strength, which might affect the enkephalin–lipid interaction.<sup>14</sup> The pH value of the solution was ca. 4.3. Liposomes were prepared essentially in the same way as described previously.<sup>20</sup> The lipid dissolved in chloroform was spread as a thin layer onto the wall of a test tube by removing the solvent with an evaporator, followed by drying under high vacuum overnight. The lipid film was hydrated under vortexing by adding the aqueous solution of enkephalin at a peptide/lipid mole ratio of 1/10. The lipid suspension was sonicated for 5–10 min at 45–60 °C using an ultrasonic generator and then centrifuged to sediment traces of light-scattering multilamellar aggregate and titanium particles from the sonicator tip probe. Aliquots of the clear supernatant were used for the Raman measurements. The pH of the final lipid suspension was ca. 4.7. In separate experiments, we prepared liposomes without enkephalin and then added aqueous enkephalin solution to the liposome suspension. Both preparation methods gave identical Raman spectra.

Model compounds of aromatic side chains, AcTyrEE and AcPheEE, were dissolved in water, methanol, chloroform, and acetonitrile-*d*<sub>3</sub> (deuterated acetonitrile was used to avoid overlap of Raman bands). As an internal standard of Raman scattering intensity, sodium perchlorate (water and methanol solutions) or tetra-*n*-butylammonium perchlorate (chloroform and acetonitrile solutions) was added.

The UVRR apparatus used in this study was described in a previous paper.<sup>21</sup> Excitation was effected by the fifth harmonics (213 nm) of an Nd:YAG laser Quanta-Ray DCR-3G) operating at 30 Hz or by the first anti-Stokes stimulated Raman radiation (240 nm) of hydrogen gas pumped by the fourth harmonics. The average laser power was ca. 1.3 mW for 213 nm or 0.7 mW for 240 nm at the sample (0.2–0.4 mL) in a spinning quartz cell. The scattered light was collected by a Cassegrain optics, dispersed with a double monochromator (Jasco CT-80D) and then

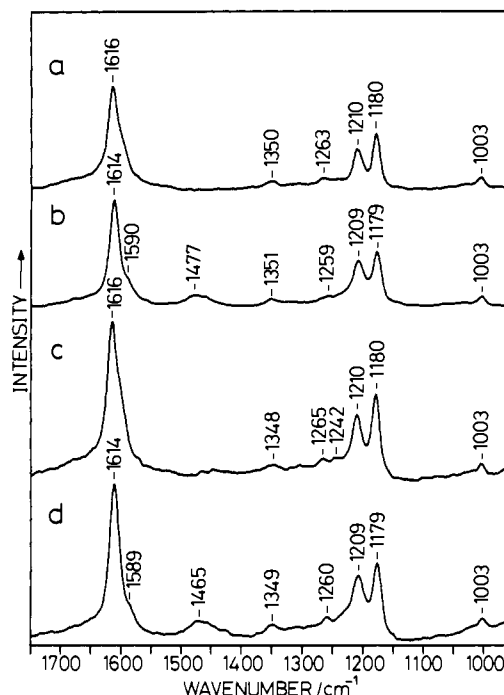


**Figure 1.** 240-nm Raman spectra of Met-enkephalin: (a) H<sub>2</sub>O solution, (b) D<sub>2</sub>O solution, and (c) DLPC liposome suspension prepared in H<sub>2</sub>O and (d) in D<sub>2</sub>O. The concentration of peptide is 3 mM and the peptide/lipid mole ratio is 1:10. The intensity scale is normalized to the 1003 cm<sup>-1</sup> Phe  $\nu_{12}$  band, which did not change in intensity compared to the water Raman band. The weak scattering around 1460 cm<sup>-1</sup> in (c) is due to the lipid C–H bending mode.

detected with a doubly intensified diode array (Princeton Instruments D/SIDA-7001/G). The spectral slit widths were 11 and 8.5 cm<sup>-1</sup> for 213- and 240-nm excitation, respectively. Wavenumber calibration was made by using the Raman bands of cyclohexanone–acetonitrile (1:1, v/v) and the peak wavenumbers of sharp Raman bands were reproducible to within  $\pm 1.5$  cm<sup>-1</sup>. No sample decomposition by laser irradiation was detected during the measurement (typically for 27 min). To improve the signal-to-noise ratio, 2–4 spectra obtained for fresh samples were accumulated. Saturation of Raman intensity due to ground-state depletion by laser pulses<sup>22,23</sup> was negligible under the experimental conditions adopted here.

Raman spectra of crystalline enkephalin were excited with 514.5-nm radiation from an Ar<sup>+</sup> laser and recorded on a scanning Raman spectrometer (Jeol 400D). Crystals of Leu-enkephalin containing extended or folded conformers were prepared from ethanol<sup>24</sup> or aqueous methanol solution.<sup>25</sup>

UV absorption spectra were recorded on a Hitachi 220A double beam spectrophotometer with 1-mm UV grade quartz cells at sample concentrations of 0.9–0.35 mM.

### Results

**Met-Enkephalin.** Figure 1a shows the 240-nm Raman spectrum of Met-enkephalin in H<sub>2</sub>O solution. The excitation wavelength is close to the 222-nm absorption due to the <sup>1</sup>L<sub>a</sub> ← <sup>1</sup>A<sub>1</sub> transition of the Tyr aromatic ring, and resonance enhancement of Tyr Raman scattering is much greater than that of Phe and amide.<sup>26,27</sup> Accordingly, most of the observed Raman bands are assignable to the Tyr side chain:<sup>27,28</sup>  $\nu_{8a}$  (ring C–C stretch) at 1616 cm<sup>-1</sup>,  $\nu_3$  (ring C–H bend) at 1350 cm<sup>-1</sup>,  $\nu_{7a'}$  (phenolic C–O stretch) at 1263 cm<sup>-1</sup>,  $\nu_{7a}$  (C <sub>$\beta$</sub> –C <sub>$\gamma$</sub>  stretch) at 1210 cm<sup>-1</sup>, and  $\nu_{9a}$  (ring C–H bend) at 1180 cm<sup>-1</sup>. Only one Phe band ( $\nu_{12}$ , ring deformation)<sup>27,29</sup>

(22) Johnson, C. R.; Ludwig, M.; Asher, S. A. *J. Am. Chem. Soc.* **1986**, *108*, 905.

(23) Su, C.; Wang, Y.; Spiro, T. G. *J. Raman Spectrosc.* **1990**, *21*, 435.

(24) Griffin, J. F.; Langs, D. A.; Smith, G. D.; Blundell, T. L.; Tickle, I. J.; Bedarkar, S. *Proc. Natl. Acad. Sci. U.S.A.* **1986**, *83*, 3272.

(25) Smith, G. D.; Griffin, J. F. *Science* **1978**, *199*, 1214.

(26) Rava, R. P.; Spiro, T. G. *J. Phys. Chem.* **1985**, *89*, 1856.

(27) Harada, I.; Takeuchi, H. In *Spectroscopy of Biological Systems*; Clark, R. J. H., Hester, R. E., Eds.; John Wiley and Sons: New York, 1986; pp 113–175.

(16) Hildebrandt, P. G.; Copeland, R. A.; Spiro, T. G.; Otlewski, J.; Laskowski, Jr. M.; Prendergast, F. G. *Biochemistry* **1988**, *27*, 5426.

(17) Su, C.; Park, Y. D.; Liu, G.-Y.; Spiro, T. G. *J. Am. Chem. Soc.* **1989**, *111*, 3457.

(18) Harada, I.; Yamagishi, T.; Uchida, K.; Takeuchi, H. *J. Am. Chem. Soc.* **1990**, *112*, 2443.

(19) Asher, S. A.; Larkin, P. J.; Teraoka, J. *Biochemistry* **1991**, *30*, 5944.

(20) Takeuchi, H.; Nemoto, Y.; Harada, I. *Biochemistry* **1990**, *29*, 1572.

(21) Takeuchi, H.; Harada, I. *J. Raman Spectrosc.* **1990**, *21*, 509.

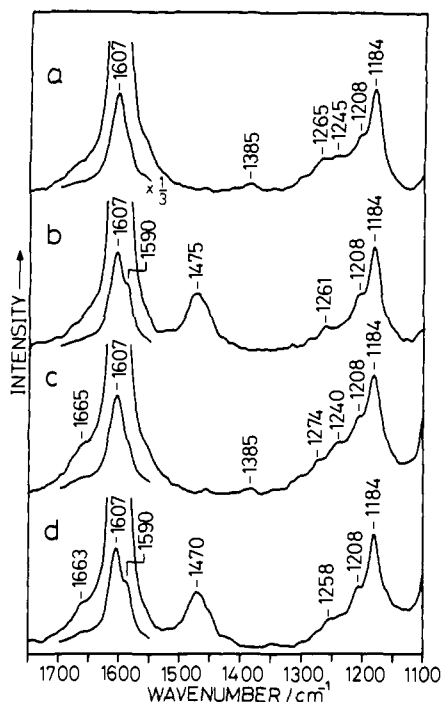


**Figure 2.** 213-nm Raman spectra of Met-enkephalin: (a) H<sub>2</sub>O solution, (b) D<sub>2</sub>O solution, and (c) DLPC liposome suspension prepared in H<sub>2</sub>O and (d) in D<sub>2</sub>O. The concentration of peptide is 3 mM, and the peptide/lipid mole ratio is 1:10. The spectra below 1100 cm<sup>-1</sup> were not recorded for liposomes because of stray light arising from strong Rayleigh scattering.

is observed at 1003 cm<sup>-1</sup>, which is the strongest of the Phe bands when excited at 240 nm.<sup>23</sup> In D<sub>2</sub>O solution (Figure 1b), a weak shoulder appears at 1590 cm<sup>-1</sup> due to Tyr  $\nu_{8b}$  (ring C-C stretch), as a result of frequency downshift upon deuteration at the phenolic hydroxyl group.<sup>28</sup> Another new band at 1477 cm<sup>-1</sup> in the D<sub>2</sub>O solution spectrum is assigned to the amide II' mode (C-N stretch) of the peptide backbone. The apparent intensity increase of the Tyr  $\nu_{9a}$  band is due to an overlap of the solvent D<sub>2</sub>O band around 1210 cm<sup>-1</sup>.

The 240-nm Raman spectrum of Met-enkephalin incorporated into DLPC liposomes (Figure 1c) differs from that in aqueous solution in some respects. A new Raman band appears at 1242 cm<sup>-1</sup> when incorporated into liposomes. This band is assignable to amide III (C-N stretch + N-H bend) because of disappearance in D<sub>2</sub>O suspension (see Figure 1d). The Tyr  $\nu_{7a}$  band at 1265 cm<sup>-1</sup> (1260 cm<sup>-1</sup> in D<sub>2</sub>O suspension) is much sharper than that in aqueous solution, though the peak frequency is close to each other. Another marked difference between the solution and liposome spectra is a large change in the intensity ratio of the Tyr Raman bands against the Phe  $\nu_{12}$  band. When the intensity scale is normalized to the peak height of the Phe band, all of the Tyr  $\nu_{8a}$ ,  $\nu_{7a}$ , and  $\nu_{9a}$  bands become ca. 50% stronger in liposomes than in aqueous solution (compare Figure 1a,c). The increase in Tyr/Phe intensity ratio is reproduced in the spectrum of liposomes prepared in D<sub>2</sub>O (Figure 1d). Examination of the Raman scattering intensity in the 1700–1000-cm<sup>-1</sup> region against the water O-H stretching band at 3400 cm<sup>-1</sup> confirmed that the Tyr/Phe relative intensity change is solely due to an increase in Tyr Raman scattering and the Phe intensity remains constant both in aqueous solution and in the lipid-bound state.

With excitation at 213 nm, the shortest wavelength available in our UVR system, Phe bands gain intensity through resonance with the L<sub>a</sub> transition at 207 nm<sup>26</sup> and become much stronger than the Tyr bands. Amide vibrational bands are also enhanced via preresonance with a  $\pi$ - $\pi^*$  (190 nm) and an  $n$ - $\sigma^*$  (160 nm)

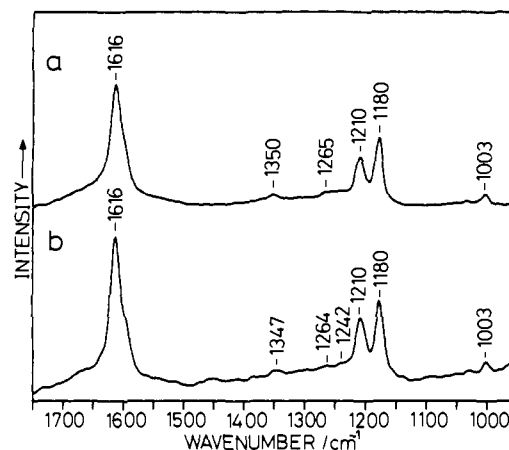


**Figure 3.** 240-nm Raman spectra of Leu-enkephalin: (a) H<sub>2</sub>O solution and (b) DLPC liposome suspension (peptide/lipid mole ratio = 1:10). The concentration of enkephalin is 3 mM. The intensity scale is normalized to the 1003 cm<sup>-1</sup> Phe  $\nu_{12}$  band.

transition.<sup>30,31</sup> Figure 2 shows the 213-nm Raman spectra of Met-enkephalin. In the H<sub>2</sub>O solution spectrum (Figure 2a), strong bands are primarily due to Phe:  $\nu_{8a}$  at 1607,  $\nu_{7a}$  at 1208, and  $\nu_{9a}$  at 1184 cm<sup>-1</sup>. A very weak shoulder around 1555 cm<sup>-1</sup> may be assigned to amide II. In D<sub>2</sub>O solution (Figure 2b), a new shoulder appears at 1590 cm<sup>-1</sup>, which is ascribed to an overlap of Phe  $\nu_{8b}$  and downshifted Tyr  $\nu_{8b}$ , one of the strongest Tyr bands with 213-nm excitation. Since the 1265-cm<sup>-1</sup> peak shows a 4-cm<sup>-1</sup> downshift on deuteration as was seen in the 240-nm spectra (1263  $\rightarrow$  1259 cm<sup>-1</sup>), it is assigned to Tyr  $\nu_{7a}$ , which becomes stronger with shorter wavelength excitation.<sup>23</sup> The amide II' mode at 1475 cm<sup>-1</sup> is much stronger than that in the 240-nm spectrum. Another new feature in the 213-nm spectrum is the broad scattering at 1385 cm<sup>-1</sup> in H<sub>2</sub>O solution. This band disappears in D<sub>2</sub>O solution and is assignable to amide S (C $\alpha$ -H bend coupled with amide III).<sup>32,33</sup> It is also noted that deuteration eliminates the 1245-cm<sup>-1</sup> band and broad scattering underlying the 1265-cm<sup>-1</sup> peak. They are assigned to amide III vibrations. No distinct Raman bands are seen in the 1700–1630-cm<sup>-1</sup> region where amide I or I' mode (mainly C=O stretch) is expected.

Met-enkephalin in DLPC liposomes gives the 213-nm Raman spectrum shown in Figure 2c. The amide S band remains at 1385 cm<sup>-1</sup>. However, amide I and III vibrations in the liposome-bound state differ from those in solution. Comparison of the liposome spectra in H<sub>2</sub>O (Figure 2c) and D<sub>2</sub>O (Figure 2d) suspension shows that liposome-bound Met-enkephalin gives two amide III bands at 1274 and 1240 cm<sup>-1</sup> in contrast to the spread bands in the aqueous solution spectrum (Tyr  $\nu_{7a}$  has no contribution to the 1274-cm<sup>-1</sup> band, because it is expected at 1265 cm<sup>-1</sup> from the 240-nm spectrum). In the amide I (I') region also, a band becomes detectable around 1665 cm<sup>-1</sup>. The appearance of the amide I band is one of the significant effects of enkephalin-liposome interactions.

**Leu-Enkephalin.** Figure 3 compares the 240-nm Raman spectra of Leu-enkephalin in H<sub>2</sub>O solution and in DLPC liposomes. The spectral features are close to those of Met-enkephalin. When bound to liposomes, the intensities of Tyr Raman bands relative to the Phe  $\nu_{12}$  1003-cm<sup>-1</sup> band again increase due to selective enhancement of Tyr scattering (the Phe band was not enhanced relative to the water O-H stretching band). However, the degree of intensity increase is small (ca. 25%) for Leu-enkephalin compared to that (ca. 50%) for Met-enkephalin. Another difference between Leu-enkephalin and Met-enkephalin is that sharpening of the Tyr  $\nu_{7a}$  band upon binding to liposomes does not occur, and the band remains practically unchanged at 1265 cm<sup>-1</sup> for Leu-enkephalin. The binding mode of Leu-enkephalin to the lipid bilayer may differ from that of Met-enkephalin to some extent as far as the Tyr side chain is concerned.

(28) Takeuchi, H.; Harada, I. *Spectrochim. Acta* **1988**, *44A*, 749.

(29) Asher, S. A.; Ludwig, M.; Johnson, C. R. *J. Am. Chem. Soc.* **1986**, *108*, 3186.

(30) Copeland, R. A.; Spiro, T. G. *Biochemistry* **1987**, *26*, 2134.

(31) Song, S.; Asher, S. A. *J. Am. Chem. Soc.* **1989**, *111*, 4295.

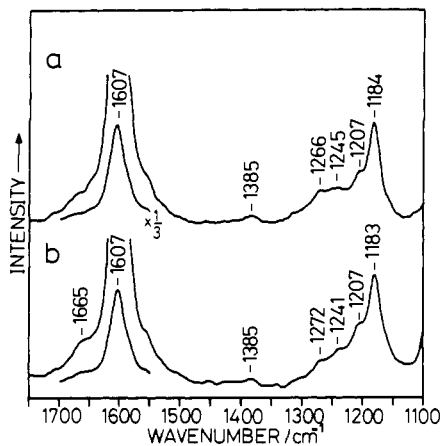


Figure 4. 213-nm Raman spectra of Leu-enkephalin: (a) H<sub>2</sub>O solution and (b) DLPC liposome suspension (peptide/lipid mole ratio = 1:10). The concentration of enkephalin is 3 mM.

The 213-nm Raman spectra of Leu-enkephalin (Figure 4) bear strong resemblance with those of Met-enkephalin. As in the case of Met-enkephalin, the amide I band of Leu-enkephalin appears at 1665 cm<sup>-1</sup> when incorporated into liposomes. The amide III band at 1245 cm<sup>-1</sup> and a broad feature extending to the Tyr  $\nu_{7a'}$  band (1266 cm<sup>-1</sup>) in H<sub>2</sub>O solution become two peaks at 1241 and 1272 cm<sup>-1</sup> in liposomes. The amide S band is seen at 1385 cm<sup>-1</sup> for both solution and liposome suspension. These amide frequencies are nearly identical to those found for Met-enkephalin, suggesting very similar backbone structure for Met- and Leu-enkephalins in each of the solution and liposome-bound states.

**Effect of Membrane Surface Charge.** Negative charges in the lipid head group region are suggested to facilitate the binding of enkephalin to the lipid micelles or liposomes.<sup>3,14</sup> Phosphatidylcholine has a negatively charged phosphate group, but the negative charge is neutralized by the positive charge of the choline group. Phosphatidylserine, on the other hand, has a net negative charge with a carboxylate group. We have prepared liposomes composed of DLPC and DPPS at a mole ratio of 4:1. Although the addition of DPPS tended to destabilize small unilamellar vesicles and make the suspension opaque, Met-enkephalin incorporated into such negatively charged liposomes gave the 213- and 240-nm Raman spectra very similar to those observed in DLPC liposomes. Amide I and III bands were clearly seen in the 213-nm Raman spectrum and the 240-nm Raman bands of the Tyr side chain showed ca. 50% intensity increase against the Phe  $\nu_{12}$  band in the presence of the liposomes. UVRR spectra of Leu-enkephalin in DLPC-DPPS liposomes were also nearly identical to those observed in DLPC liposomes. Although the content of DPPS was comparable to that found in the living cell membranes,<sup>34</sup> the surface negative charge did not affect the binding mode of enkephalin significantly. We attempted to further increase the DPPS content as employed in previous NMR studies.<sup>3,14</sup> However, higher content of DPPS accelerated the aggregation of vesicles, which caused strong diffuse scattering of the laser light and reduced the signal-to-noise ratio of the Raman spectra unacceptably.

**Solvent Effects on the Raman Scattering Intensity of Model Compounds.** The 240-nm Raman spectra of enkephalins have shown that interaction with phospholipid liposomes results in a significant increase of Raman scattering intensity of the Tyr side chain but not of the Phe side chain. In order to clarify the origin of this intensity increase, we have measured 240-nm Raman spectra of model compounds dissolved in several solvents. Figure 5 compares the Raman spectra of AcTyrEE in water, methanol, chloroform, and acetonitrile. The intensity scale of the spectra is normalized to the 933-cm<sup>-1</sup> band of perchlorate ion, which was added as an intensity standard at a AcTyrEE/perchlorate mole ratio of 1/15. The Raman bands at 1616 ( $\nu_{8a}$ ), 1210 ( $\nu_{7a}$ ), and 1180 cm<sup>-1</sup> ( $\nu_{9a}$ ) of the Tyr phenolic ring become stronger by ca. 80 and 100% in methanol and chloroform solutions, respectively, than in aqueous solution, whereas such an obvious intensity change

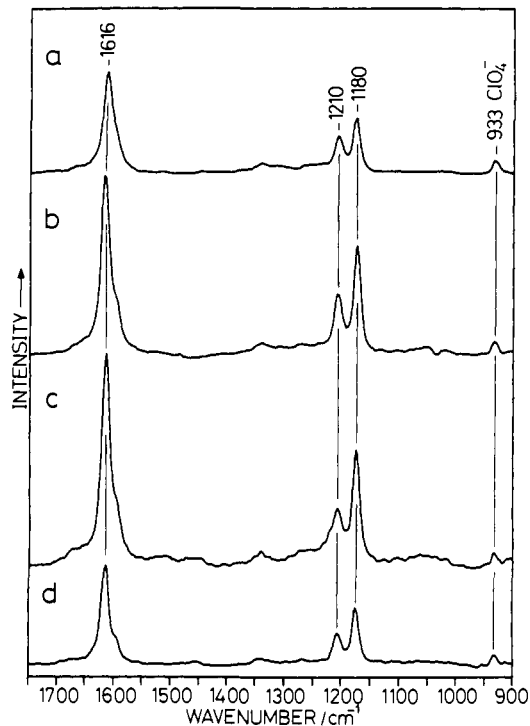


Figure 5. Solvent effects on the 240-nm Raman bands of AcTyrEE. Solvent: (a) H<sub>2</sub>O, (b) methanol, (c) chloroform, and (d) acetonitrile-*d*<sub>3</sub>. The concentration is 3 mM for H<sub>2</sub>O solution and 10 mM for the other solutions. The intensity scale is normalized to the peak height of the 933-cm<sup>-1</sup> band due to perchlorate added as an internal standard. The AcTyrEE/perchlorate mole ratio is 1/15. The solvent spectra recorded separately are subtracted from the solution spectra. Poor S/N ratios in some wavenumber regions are due to overlap of strong solvent bands.

is not seen in acetonitrile solution.

The excitation wavelength (240 nm) of the AcTyrEE Raman spectra falls on the long wavelength tail of the Tyr L<sub>a</sub> absorption and the Raman intensity is considered to come mainly through resonance with the L<sub>a</sub> transition. There are several factors that affect resonance Raman cross section.<sup>35</sup> One of them is the modification of macroscopic electric field of the incident radiation caused by solvent polarization (so-called local field effect). However, this factor can be neglected in the present experiments, because we measure the relative intensity of AcTyrEE against the internal intensity standard, both of which experience virtually the same electric field. Other factors include the magnitude of transition moment, the lifetime of the excited electronic state, and the difference between the transition energy and the incident photon energy. These three factors also affect the absorption intensity at the excitation wavelength and an increase in absorptivity is expected to increase the resonance Raman cross section. Hence, the observed Raman intensity variation may be related to the solvent perturbation on the L<sub>a</sub> absorption.

Figure 6a shows the UV absorption spectra of AcTyrEE dissolved in water, methanol, chloroform, and acetonitrile (spectrum below 235 nm was unmeasurable in chloroform solution because of strong solvent absorption). The  $\lambda_{max}$  of the L<sub>a</sub> transition shifts from 222 nm in water to 225 nm in methanol and the 3-nm red shift results in a 60% increase of the molar extinction coefficient at 240 nm ( $\epsilon_{240}$ ). Further increase in  $\epsilon_{240}$  is evident in chloroform, suggesting a larger red shift. Thus, the increase of the Raman

(32) Wang, Y.; Purrello, R.; Jordan, T.; Spiro, T. G. *J. Am. Chem. Soc.* **1991**, *113*, 6359.

(33) The Raman band that appears around 1390 cm<sup>-1</sup> in UVRR spectra of peptides and proteins was once ascribed to an overtone of amide V (Krimm, S.; Song, S.; Asher, S. A. *J. Am. Chem. Soc.* **1989**, *111*, 4290). Here we adopt a new assignment (amide S) proposed in ref 32. In either assignment, the 1390-cm<sup>-1</sup> band is a marker of nonhelical peptide structure.

(34) Devaux, P. F.; Seigneuret, M. *Biophys. Biochem. Acta* **1985**, *104*, 63.

(35) Myers, A. B.; Mathies, R. A. In *Biological Application of Raman Spectroscopy*; Spiro, T. G., Ed.; John Wiley and Sons: New York, 1987; Vol. 2, pp 1-58.

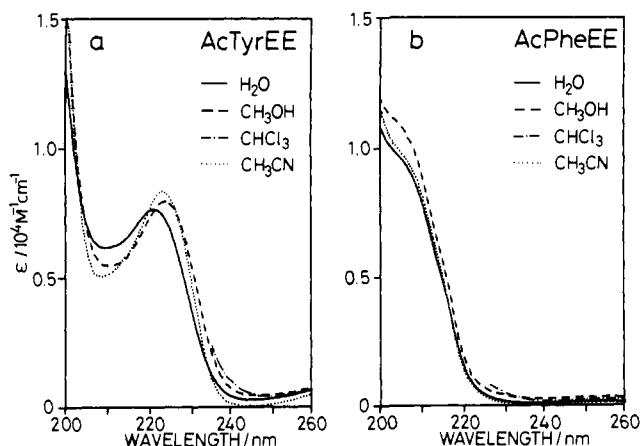


Figure 6. UV absorption spectra of (a) AcTyrEE and (b) AcPheEE in H<sub>2</sub>O, methanol, chloroform, and acetonitrile solutions. For chloroform solution, the spectrum below 235 nm was not measurable because of the solvent absorption.

scattering intensity in methanol and chloroform solutions correlates with the red shift of the L<sub>a</sub> transition and the resultant increase in  $\epsilon_{240}$ . Similar red shifts of the L<sub>a</sub> transition were reported to be induced by ethylene glycol and urea, which were considered to provide hydrophobic environments around the Tyr phenolic ring.<sup>36,37</sup> In acetonitrile solution, on the other hand, the  $\lambda_{\max}$  shifts to the red by 2 nm but  $\epsilon_{240}$  rather decreases due to sharpening of the absorption band. Possibly, the red shift and the decrease in  $\epsilon_{240}$  cancel each other out, and the 240-nm Raman cross section in acetonitrile solution does not differ from that in aqueous solution.

Figure 7 shows the 240-nm Raman spectra of AcPheEE in the same solvent system as employed for AcTyrEE. The AcPheEE/perchlorate mole ratio (2/3) is increased to ten times that for AcTyrEE because Phe is a weak scatterer at 240 nm. The Phe  $\nu_{12}$  band at 1004 cm<sup>-1</sup> shows ca. 50 and 20% intensity increase in methanol and chloroform, respectively, compared to that in water, while no significant increase is seen for acetonitrile solution. The solvent effects on the  $\nu_{12}$  Raman intensity of AcPheEE are analogous to those observed for  $\nu_{8a}$ ,  $\nu_{7a}$ , and  $\nu_{9a}$  of AcTyrEE. Less polar solvents (methanol and chloroform) give stronger Raman scattering than the polar solvents (water and acetonitrile). The UV absorption of AcPheEE at 240 nm is very weak in water and acetonitrile because the L<sub>a</sub> transition at 207 nm is far away from this wavelength. As shown in Figure 6b, the solvent change from water to methanol intensifies the L<sub>a</sub> absorption by about 10% and shifts the  $\lambda_{\max}$  to the red slightly with a concomitant increase in  $\epsilon_{240}$ . Similar but less increase in  $\epsilon_{240}$  is seen for chloroform solution attributable to a composite effect of red-shifting and band sharpening. Thus the Raman intensity variation of Phe  $\nu_{12}$  also correlates with the UV absorption change. The present result is consistent with the observation that ethylene glycol, when added to aqueous Phe solution, produces a red shift of the L<sub>a</sub> transition<sup>36,37</sup> and a marked intensification of the Phe  $\nu_{12}$  band with 229-nm excitation.<sup>16</sup>

Solute-solvent interaction must be responsible for the red shift and the sharpening of the L<sub>a</sub> absorption band, which are closely related to the change in  $\epsilon_{240}$  and the 240-nm Raman intensity enhancement as described above. Solvent-induced red shifts are usually accounted for in terms of dipole-dipole, dipole-polarization (including transition dipole), and hydrogen-bonding interactions between the solute and solvent.<sup>38</sup> The absorption band shape may also be affected by such interactions, in a time-dependent and hence more complicated way than is the transition energy. Of the possible solute-solvent interactions, hydrogen bonding is unlikely the main origin of the spectral changes observed here, because both methanol and chloroform cause analogous solvent

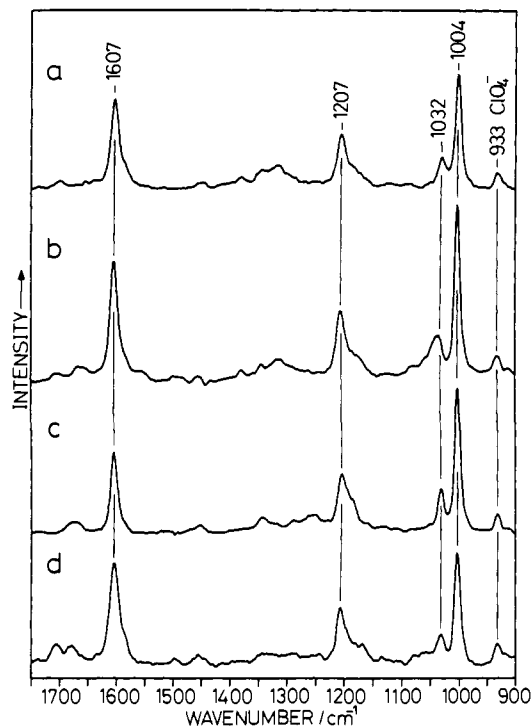


Figure 7. Solvent effects on the 240-nm Raman bands of AcPheEE. Solvent: (a) H<sub>2</sub>O, (b) methanol, (c) chloroform, and (d) acetonitrile-*d*<sub>3</sub>. The concentration is 20 mM for H<sub>2</sub>O solution and 100 mM for the others. The intensity scale is normalized to the peak height of the 933-cm<sup>-1</sup> band of perchlorate added as an internal standard. The AcPheEE/perchlorate mole ratio is 2/3. The solvent bands are subtracted.

effects for AcTyrEE, whose hydroxyl group forms hydrogen bonds with methanol but not with chloroform. Dipole-dipole and/or dipole-polarization interactions must be responsible for the spectral changes. Possibly, balance of such dipole interactions determines the degree of intensity enhancement. The fact that the intensity enhancement of AcPheEE in chloroform is not so large as expected from the data for AcTyrEE may indicate that the balance of interaction forces depends on the electric properties not only of the solvent but also of the solute, the Phe ring being nearly nonpolar, whereas the Tyr ring being polar. Although the exact mechanism of the intensity enhancement is unclear at present, the 240-nm Raman intensity increases in solvents less polar than water, at least for Tyr and Phe aromatic ring modes.

The Raman intensities of AcTyrEE and AcPheEE were examined also with 213-nm excitation in water, methanol, and acetonitrile solutions. The scattering intensity from both aromatic rings did not change by more than 20% on going from aqueous to methanol or acetonitrile solution. Changes in  $\epsilon_{213}$  were also less than 20% (see Figure 6). Tyr and Phe in water absorb the 213-nm radiation strongly, and organic solvents produce rather small relative changes in  $\epsilon_{213}$  against the "standard" value in water. In weakly absorbing regions, such as at 240 nm, solvent perturbation produces a large relative change against the small  $\epsilon_{240}$  value in water, and the 240-nm Raman intensity also changes largely relative to that in aqueous solution. This may be the reason why the 240-nm Raman intensity is a good probe of the environmental changes of Tyr and Phe side chains, e.g., from aqueous to hydrophobic environments.

## Discussion

**Backbone Structure.** In the 213-nm Raman spectra of aqueous solutions of Met- and Leu-enkephalins, the amide III modes gave broad Raman scattering around 1245–1265 cm<sup>-1</sup>, suggesting irregular backbone structure and the amide CO groups hydrogen-bonded with water.<sup>27</sup> The amide S band observed at 1385 cm<sup>-1</sup> shows that nonhelical structure is one of the major conformations of the peptide.<sup>32</sup> When a peptide takes a single irregular structure with CO hydrogen bonding, an amide I band is expected in the 1670–1660-cm<sup>-1</sup> region.<sup>27</sup> However, no distinct

(36) Donovan, J. W. *J. Biol. Chem.* **1969**, *244*, 1961.

(37) A'zary, E. P.; Bigelow, C. C. *Can. J. Biochem.* **1970**, *48*, 953.

(38) Bayliss, N. S.; McRae, E. G. *J. Phys. Chem.* **1954**, *58*, 1002.

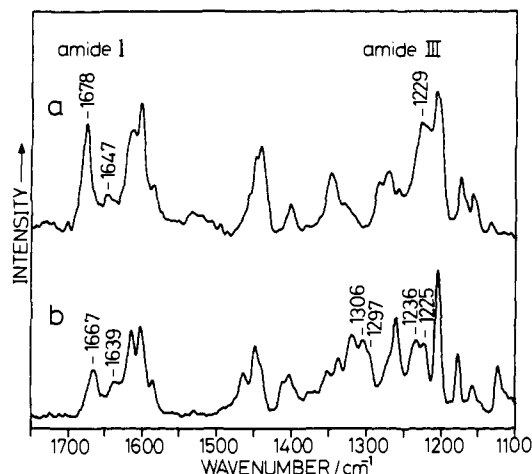


**Figure 8.** Visible (514.5 nm) Raman spectra of Leu-enkephalin crystals: (a)  $\beta$ -sheet structure crystallized from ethanol<sup>24</sup> and (b)  $\beta$ -turn structure crystallized from aqueous methanol.<sup>25</sup> Peak wavenumbers are given only for amide I and III bands, which shifted upon N-deuteration.

Raman bands are found in that frequency region, nor any other regions where amide I bands characteristic of various secondary structures usually appear. Han et al. reported nonresonant Raman spectra of Leu-enkephalin in H<sub>2</sub>O and D<sub>2</sub>O solutions with visible radiation excitation.<sup>39</sup> They found a broad amide III band at 1248 cm<sup>-1</sup> in H<sub>2</sub>O solution and a very broad amide I' band extending from 1700 to 1630 cm<sup>-1</sup> in D<sub>2</sub>O solution. The absence of any distinct amide I (I') band in the present UVRR spectra is consistent with the broad feature of the amide I' band in the visible Raman spectrum. Multiple irregular conformers with diverse amide I frequencies in aqueous solution must spread the Raman scattering intensity over a wide frequency range, and individual Raman bands are smeared out by the tail of a strong Phe band in the 213-nm Raman spectra. The amide I vibration is accompanied by a large change of electric dipole moment, and dipole-dipole interactions among the residues change the frequency depending on the relative orientation of the C=O groups.<sup>40</sup> Thus, the variety in secondary structure is reflected sensitively in the bandwidth of amide I. On the other hand, the amide III frequency is largely affected by hydrogen bonding at the amide NH, and its bandwidth reflects the distribution in the strength of hydrogen bonding. It is reasonable to conclude that both Met-enkephalin and Leu-enkephalin exist in aqueous solution as an ensemble of different conformers with irregular backbone structures. The equilibrium of various conformers in aqueous solution has been probed by NMR,<sup>41,42</sup> visible Raman,<sup>39</sup> and circular dichroism<sup>43</sup> studies.

In the liposome-bound state, enkephalin gives one amide I band at 1665 cm<sup>-1</sup>, two amide III bands at 1275 and 1240 cm<sup>-1</sup>, and the amide S band at 1385 cm<sup>-1</sup>. The appearance of the amide I band indicates that conformational diversity of enkephalin in aqueous solution reduces significantly in liposomes, possibly to a single conformer. The amide I frequency and the appearance of amide S band exclude the possibility of  $\alpha$ -helical structure.<sup>27,32</sup> A  $\beta$ -sheetlike extended or irregularly folded conformer may exist in the liposome.

We have recorded the visible Raman spectra of two Leu-enkephalin crystals, for which X-ray studies have shown that the pentapeptide takes  $\beta$ -sheet and  $\beta$ -turn conformations, respectively.<sup>24,25</sup> Crystals of N-deuterated Leu-enkephalin have also been examined to identify the amide I and III bands. Figure 8

shows the Raman spectra of the non-deuterated crystals. The  $\beta$ -sheet conformation is characterized by a dominant amide I band at 1678 cm<sup>-1</sup> and a single strong amide III band at 1229 cm<sup>-1</sup> (Figure 8a). On the other hand, the  $\beta$ -turn conformation gives strong 1667-cm<sup>-1</sup> and weak 1639-cm<sup>-1</sup> amide I bands with weaker amide III bands in the 1310–1290- and 1240–1220-cm<sup>-1</sup> regions (Figure 8b). The splitting of amide III mode to multiple components is ascribed to heterogeneity in the N–H hydrogen bonding strength, which is inevitable in folded conformations. The high (~1300 cm<sup>-1</sup>) and low (~1230 cm<sup>-1</sup>) frequency components are due to strong intramolecular hydrogen bonding and weak or no hydrogen bonding, respectively, at the amide N–H sites.

Comparison of the UVRR spectra of the lipid-bound enkephalin with the visible Raman spectra of the crystals provides an insight into the backbone structure of enkephalin. The amide I band (1665 cm<sup>-1</sup>) observed for liposome-bound enkephalins is much closer in frequency to the 1667-cm<sup>-1</sup> band of  $\beta$ -turn than to the 1678-cm<sup>-1</sup> band of  $\beta$ -sheet. Further, two amide III bands at ca. 1275 and 1240 cm<sup>-1</sup> in the liposome-bound state corresponds to the two groups of amide III modes around 1300 and 1230 cm<sup>-1</sup> of the  $\beta$ -turn conformation. Therefore, it is very likely that enkephalin takes a folded conformation when bound to lipid membranes. However, the folded conformation may not be exactly the  $\beta$ -turn conformation that was found in the crystal, because the high-frequency component of amide III is significantly lower than that of the  $\beta$ -turn structure, suggesting much weaker intramolecular N–H...O=C hydrogen bonding due to a different folding pattern.

**Environments of Tyr and Phe Side Chains.** The solvent effects on the Raman spectra of AcTyrEE and AcPheEE have demonstrated that the 240-nm Raman scattering intensity of Tyr ( $\nu_{8a}$ ,  $\nu_{7a}$ ,  $\nu_{9a}$ ) and Phe ( $\nu_{12}$ ) becomes stronger in less polar environments. The bilayer of a liposome is composed of polar head group region and nonpolar hydrophobic interior. Another coexisting environment is the aqueous phase around the bilayer surface. Aqueous solution corresponds to the aqueous phase. The solvation by acetonitrile, having a very large dipole moment, may mimic the environment in the lipid polar head group region. The hydrophobic environment in the bilayer interior may be close to that afforded by methanol or chloroform. Accordingly, the Raman scattering intensity of Tyr or Phe is expected to be particularly large when the side chain is located in the bilayer hydrophobic interior, whereas it will be as small as in aqueous or acetonitrile solution for the residue located in the aqueous phase or the polar head group region. In aqueous solution, enkephalin takes an ensemble of various main-chain conformations, and the Tyr and Phe side chains are, of course, exposed to the solvent water. Thus, the intensity ratio of the Tyr Raman bands to the Phe band is close to that expected from those of AcTyrEE and AcPheEE in aqueous solution. In the liposome-bound state, on the other hand, the Tyr Raman bands are selectively enhanced (by 50% for Met-enkephalin and 25% for Leu-enkephalin) against the Phe band. This observation evidences that the phenolic ring of Tyr at position 1 is buried, at least partly, in the hydrophobic interior of the liposome bilayer, and the degree of insertion is greater for Met-enkephalin than for Leu-enkephalin. In contrast, the Phe side chain at position 4 is likely to be exposed to the aqueous phase or located in the polar head group region.

The interaction of the Tyr side chain with the lipid environments is also reflected in the frequency and band shape of the Tyr  $\nu_{7a}$  mode. Sharpening of the  $\nu_{7a}$  band was observed for Met-enkephalin on going from aqueous solution to liposome-bound state. Such sharpening occurs when the phenolic OH is not hydrogen-bonded with proton donors.<sup>44</sup> According to the relationship between the  $\nu_{7a}$  frequency and the state of hydrogen bonding,<sup>44</sup> the observed frequency (1265 cm<sup>-1</sup>) suggests that the Tyr phenolic OH of Met-enkephalin is weakly hydrogen-bonded to a proton acceptor when bound to liposomes. It is likely that the body of the Tyr phenolic ring is mostly buried in the lipid hydrophobic

(39) Han, S.-L.; Stimson, E. R.; Maxfield, F. R.; Scheraga, H. A. *Int. J. Peptide Protein Res.* **1980**, *16*, 173.

(40) Krimm, S. In *Biological Application of Raman Spectroscopy*; Spiro, T. G., Ed.; John Wiley and Sons: New York, 1987; Vol. 1, pp 1–45.

(41) Higashijima, T.; Kobayashi, J.; Nagai, U.; Miyazawa, T. *Eur. J. Biochem.* **1979**, *97*, 43.

(42) Motta, A.; Tancredi, T.; Temussi, P. A. *FEBS Lett.* **1987**, *215*, 215.

(43) Spirtes, M. A.; Schwartz, R. W.; Mattice, W. L.; Coy, D. H. *Biochem. Biophys. Res. Commun.* **1978**, *81*, 602.

(44) Takeuchi, H.; Watanabe, N.; Satoh, Y.; Harada, I. *J. Raman Spectrosc.* **1989**, *20*, 233.

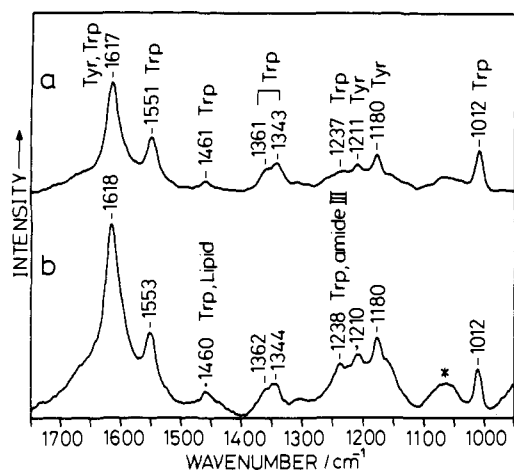


**Figure 9.** 240-nm Raman spectra of  $[\text{Trp}^4]\text{Met-enkephalin}$ : (a)  $\text{H}_2\text{O}$  solution and (b) DLPC liposome suspension (peptide/lipid mole ratio = 1:10). The concentration of enkephalin is 1 mM. The intensity scale is normalized to the  $1012\text{-cm}^{-1}$  Trp band. The band marked with \* and the broad feature underlying the  $1250\text{--}1150\text{-cm}^{-1}$  region of spectrum b are due to the quartz cell.

region, but the exocyclic OH group is hydrogen-bonded to an oxygen atom of the acyl-glycerol ester linkage in the boundary of hydrophobic region. For Leu-enkephalin, on the other hand, no sharpening was observed, and the  $\nu_{7a'}$  band in the liposome-bound state was as broad as that in aqueous solution. The peak frequency was also practically identical in both states. These observations suggest that the Tyr side chain of Leu-enkephalin is located in a more hydrophilic region with the OH group being hydrogen-bonded with water molecules. Thus, the Tyr hydrogen bonding state suggested by the  $\nu_{7a'}$  band frequency and shape is consistent with the environmental hydrophobicity of this N-terminal residue indicated by the 240-nm Raman intensity increase.

In order to obtain further information on the environment of aromatic side chain at position 4, we have measured the UVRR spectra of an enkephalin analog,  $[\text{Trp}^4]\text{Met-enkephalin}$ , which has a receptor affinity comparable to that of Met-enkephalin.<sup>45</sup> The amide I and III bands observed in the 213-nm Raman spectra have shown that this analog also takes a folded conformer in liposomes (spectra not shown). The Trp side chain replacing the Phe absorbs UV radiation strongly, and the Raman spectra provide direct structural information on the Trp side chain. Figure 9 compares the 240-nm Raman spectra of  $[\text{Trp}^4]\text{Met-enkephalin}$  in  $\text{H}_2\text{O}$  solution and in DLPC liposomes. The intensity ratio of the  $1360/1340\text{-cm}^{-1}$  doublet due to Trp is known as a sensitive marker of hydrophobic interaction with the environment: the stronger the interaction, the higher the intensity ratio.<sup>46</sup> This correlation applies in 240-nm excited spectra as well as in visible Raman spectra.<sup>18</sup> In the  $\text{H}_2\text{O}$  solution spectrum (Figure 9a), the high frequency component of the doublet is much weaker than the low frequency one, indicative of the absence of hydrophobic interaction in  $\text{H}_2\text{O}$  solution. This intensity ratio remains unchanged practically in the liposome spectrum (Figure 9b). The Trp side chain of  $[\text{Trp}^4]\text{Met-enkephalin}$  must be exposed in the hydrophilic surface region of the lipid bilayer but not buried in the hydrophobic region. This observation suggests that the Phe side chain of natural enkephalins is also exposed in the membrane surface.

The  $1617\text{-cm}^{-1}$  band of  $[\text{Trp}^4]\text{Met-enkephalin}$  is due to Tyr  $\nu_{8a}$  with a contribution from a Trp vibration around  $1620\text{ cm}^{-1}$ . The intensity of this band relative to the bands due solely to Trp (for example, the  $1551\text{-}$  and  $1012\text{-cm}^{-1}$  bands) increases by about 50% in liposomes compared to that in  $\text{H}_2\text{O}$  solution. Since the environment of the Trp side chain is nearly the same in both states as judged from the  $1360\text{--}1340\text{-cm}^{-1}$  doublet intensity, it is unlikely

that the underlying  $1620\text{-cm}^{-1}$  band of Trp gains intensity when the peptide is bound to liposomes. Thus the intensity increase of the  $1617\text{-cm}^{-1}$  band is ascribed to Tyr. Other Tyr bands at  $1180$  and  $1211\text{ cm}^{-1}$  also become stronger by about 40%. The intensity increase of Tyr Raman bands parallels that observed for natural enkephalins, indicating that the Tyr side chain of  $[\text{Trp}^4]\text{Met-enkephalin}$  is also buried in the bilayer hydrophobic region.

The intensity increase of Tyr Raman bands when bound to liposomes is in the order of Met-enkephalin  $\approx$   $[\text{Trp}^4]\text{Met-enkephalin}$   $>$  Leu-enkephalin. The opioid receptor affinity measured by  $^3\text{H}$ naloxone displacement from rat brain membrane preparations is also comparable for Met-enkephalin and  $[\text{Trp}^4]\text{Met-enkephalin}$ , but it is much smaller for Leu-enkephalin.<sup>45</sup> The insertion of the N-terminal Tyr side chain into the bilayer hydrophobic region seems to be important in efficient binding to receptors. It is known that the N-terminal portion of enkephalin is essential to the activity, and any modification of the Tyr residue leads to drastic loss of activity.<sup>2</sup> The hydrophobic environment provided by lipid membranes may play a role in protecting the N-terminal Tyr from degradation, which is usually caused by aminopeptidases in the tissues and is an important factor to determine the activity of peptides.<sup>47</sup> In sharp contrast to Tyr, the side chain of the fourth residue, Phe or Trp, is exposed to the surface of the bilayer. This observation may be related to the fact that the activity is rather insensitive to the modification at this residue position.<sup>48</sup> It is probable that the contrasting locations of the aromatic side chains in the membrane have significance not only in increasing the receptor affinity but also in keeping the activity. Actually, Met-enkephalin has not only higher affinity but also higher activity than Leu-enkephalin.<sup>49</sup> The higher activity of Met-enkephalin may partly be ascribed to higher protection from degradation.

**Comparison with Previous Results.** Behnam and Deber<sup>12</sup> proposed a model for the lipid-bound conformer on the basis of  $^1\text{H}$ - and  $^{13}\text{C}$ -NMR data on Met- and Leu-enkephalins in lysophosphatidylcholine micelles. The model has a  $\beta$ -turn backbone structure with both Tyr and Phe side chains partly embedded in the lipid matrix. Photochemically induced dynamic nuclear polarization experiments by Zetta et al.<sup>11</sup> showed that the Tyr side chain of Met-enkephalin is not fully exposed to the aqueous phase in a similar micelle system. An FT-IR study by Surewicz and Mantsch<sup>15</sup> suggested that natural enkephalins take a hydrogen-bonded turn structure in the environments of neutral lipid bilayers, though no information on the environments of side chains was obtained. Recently, the TRNOE method was employed by Milon et al.<sup>14</sup> to analyze the conformations of Leu-enkephalin and its analogs in the presence of phosphatidylcholine/phosphatidylserine (1:1) liposomes. They concluded that active peptides adopt an identical folded conformation with the Tyr side chain exposed to the aqueous phase. All the previous studies proposed that enkephalin binds to phospholipids with a folded conformation, which is consistent with our UVRR conclusion. However, there are discrepancies among the previous and present conclusions for the mode of interaction of the Tyr and Phe side chains with the lipid environments. Particularly, the result of the TRNOE study appears to contradict our UVRR result.

In the TRNOE experiments, enkephalin was added to the negatively charged liposomes at a peptide/lipid mole ratio of 1:1. TRNOE works for peptides in a fast exchange between the lipid-bound and free states but not for tightly bound peptides. Thus, the mode of interaction revealed by the TRNOE analysis concerns the weakly bound peptides. Weakly bound peptides may be located on the membrane surface via electrostatic interactions. Actually, addition of negatively charged lipid and a high pep-

(47) Kosterlitz, H. W.; Lord, J. A.; Paterson, S. J.; Waterfield, A. A. *Br. J. Pharmacol.* **1980**, *68*, 333.

(48) Hansen, P. E.; Morgan, B. A. In *The Peptides*; Udenfriend, S., Meienhofer, J., Eds.; Academic Press: Orlando, FL, 1984; Vol. 6, pp 269–321.

(49) Paterson, S. J.; Robson, L. E.; Kosterlitz, H. W. In *The Peptides*; Udenfriend, S., Meienhofer, J., Eds.; Academic Press: Orlando, FL, 1984; Vol. 6, pp 147–190.

(45) Schiller, P. W.; St-Hilaire, J. *J. Med. Chem.* **1980**, *23*, 290.

(46) Harada, I.; Miura, T.; Takeuchi, H. *Spectrochim. Acta* **1986**, *42A*, 307.

tide/lipid ratio were necessary to observe sufficient TRNOE signals.<sup>14</sup> In the present UVRR experiments, on the other hand, enkephalin was mixed with neutral lipid at 1:10 mole ratio. Since TRNOE signal was very weak in the absence of charged lipids, contribution of weakly bound species to the UVRR spectrum may be neglected. Free peptides in the aqueous phase cannot be the major component either, because UVRR spectra showed large changes in the amide and aromatic side chain vibrations on going from aqueous solution to the peptide-liposome mixture. Accordingly, the binding mode of enkephalin revealed by the present UVRR experiments concerns the tightly bound peptides, which are the major component at low peptide/lipid ratios. The formation of tightly bound complex may account for the observation that NMR signals got broader and the signal-to-noise ratio of TRNOE signals decreased with increasing amount of the lipid added to the enkephalin solution.<sup>14</sup> A chromatographic study suggested the presence of tightly bound enkephalin, which remained bound even after gel filtration.<sup>50</sup> In living cells, enkephalin is likely to bind to the cell membrane in two steps. The initial step is weak binding to the cell surface through electrostatic interaction, and the next step is tight binding through hydrophobic interaction.

(50) Cherubini, O.; De Marco, V.; Roscetti, G.; Possenti, R.; Roda, L. G. *Int. J. Peptide Protein Res.* **1984**, *23*, 435.

## Conclusions

Met-enkephalin and Leu-enkephalin exist as an ensemble of various extended conformers in aqueous solution. In the liposome-bound state, the peptide backbone takes a folded conformation predominantly. The Tyr side chain of Met-enkephalin is mostly inserted into the hydrophobic region of the lipid bilayer with its phenolic hydroxyl group hydrogen-bonded with a proton acceptor of the lipid, whereas the Phe side chain is located in the polar head group region or exposed to the aqueous phase. For Leu-enkephalin, the Tyr side chain is less buried in the membrane than for Met-enkephalin and the hydroxyl group is hydrogen-bonded with water. [Trp<sup>4</sup>]Met-enkephalin also has a folded main-chain conformation in the membrane-bound state, and the Tyr and Trp side chains are located in the hydrophobic and hydrophilic regions, respectively, in a manner similar to the corresponding side chains of Met-enkephalin. The hydrophobicity of the Tyr environment in the membrane-bound state correlates with the receptor affinity and opiate activity. UVRR spectroscopy proves to be a useful tool for investigating the environments of aromatic side chains of membrane-bound peptides.

**Acknowledgment.** This work is supported by a Grant-in-Aid for General Scientific Research (No. 01470142) from the Ministry of Education, Science, and Culture and by a Grant-in-Aid from The Tokyo Biochemical Research Foundation.

## Conformational Analysis of Cyclic Hexapeptides Containing the D-Pro-L-Pro Sequence To Fix $\beta$ -Turn Positions

John W. Bean, Kenneth D. Kopple,\* and Catherine E. Peishoff

Contribution from the Department of Physical and Structural Chemistry, L-940, SmithKline Beecham Pharmaceuticals, P.O. Box 1539, King of Prussia, Pennsylvania 19406.

Received December 2, 1991

**Abstract:** Two cyclic hexapeptides, cyclo(D-Pro-Pro-Gly-Arg-Gly-Asp) (**1**) and cyclo(D-Pro-Pro-Arg-Gly-Asp-Gly) (**2**), containing a D-Pro-Pro sequence introduced to define and fix the phase of a two- $\beta$ -turn backbone were examined by proton NMR methods. The NMR data were used in constrained distance geometry conformation searches to identify the probable backbone conformations. The conformation searches were conducted using upper and lower bound constraints derived from observed nuclear Overhauser effects (NOEs) involving backbone protons and also using additional lower bound constraints from backbone and  $\beta$ -proton NOEs judged to be unobserved. The two procedures gave substantially the same results although the dihedral angle ranges were narrower with the additional constraints. In each case, the D-Pro-Pro sequence unequivocally adopted a type II'  $\beta$ -turn conformation as anticipated and stabilized the second turn across the ring from it. In the case of the Arg-Gly sequence of **1**, a type II turn was predominant; for the Gly-Asp sequence of **2**, structures with type I, II, II', and III turns were all returned by the constrained search, and there were no experimental grounds to suggest a preference.

## Introduction

Synthetic cyclic peptides of stable backbone conformation can be tools for mapping the biologically active conformations of peptide sequences and, thus, an intermediate step on the path from polypeptide to peptidomimetic. We describe here the conformational component of one such study, in which two successive proline residues are used to limit the conformational freedom of cyclic hexapeptides.

The two- $\beta$ -turn backbone conformation of cyclic hexapeptides and the ability of proline residues to define its phase by occupying the  $i + 1$  position of one of the turns are both well documented,<sup>1-15</sup>

as is the preference of proline for the  $i + 1$  position of  $\beta$ -turns in proteins.<sup>16</sup> The principal conformation-determining feature of proline is the pyrrolidine ring-induced restriction of the backbone dihedral angle  $\phi$  to the 50–90° ranges, the sign being negative

(7) Kessler, H.; Matter, H.; Gemmecker, G.; Kling, A.; Kottenhahn, M. *J. Am. Chem. Soc.* **1991**, *113*, 7550–7563.

(8) Karle, I. L.; Chiang, C. C. *Acta Crystallogr.* **1984**, *C40*, 1381–1386.

(9) Chiang, C. C.; Karle, I. L.; Wieland, T. *Int. J. Pept. Protein Res.* **1982**, *20*, 414–420.

(10) Declercq, J.-P.; Tinant, B.; Bashwira, S.; Hootel , C. *Acta Crystallogr.* **1990**, *C46*, 1259–1262.

(11) Cyclo(D-Pro-Gly-Pro-Arg-Gly-Asp), examined by NMR in this laboratory, is closely analogous. Peishoff, C. E.; Ali, F. A.; Bean, J. W.; Calvo, R.; D'Ambrosio, C. A.; Eggleston, D. S.; Kline, T. P.; Koster, P. F.; Nichols, A.; Powers, D.; Romoff, T.; Samanen, J. M.; Stadel, J.; Vasko, J. A.; Wong, A.; Kopple, K. D. *J. Med. Chem.*, submitted for publication.

(12) Schwyzer, R.; Ludescher, U. *Helv. Chim. Acta* **1969**, *52*, 2033–40.

(13) Schwyzer, R.; Grathwohl, C.; Meraldi, J. P.; Tun-Kyi, A.; Vogel, R.; Wuethrich, K. *Helv. Chim. Acta* **1972**, *55*, 2545–2549.

(14) Gierasch, L. M.; Deber, C. M.; Madison, V.; Niu, C.-H.; Blout, E. R. *Biochemistry* **1981**, *20*, 4730–4738.

(15) Kopple, K. D.; Schamper, T. J.; Go, A. *J. Am. Chem. Soc.* **1974**, *96*, 2597–2605.

(16) Chou, P. Y.; Fasman, G. D. *J. Mol. Biol.* **1977**, *115*, 135–175.

(1) Kostansek, E. C.; Thiessen, W. E.; Schomburg, D.; Lipscomb, W. N. *J. Am. Chem. Soc.* **1979**, *101*, 5811–5815.

(2) Kostansek, E. C.; Lipscomb, W. N.; Thiessen, W. E. *J. Am. Chem. Soc.* **1979**, *101*, 834–837.

(3) Brown, J. N.; Yang, C.-H. *J. Am. Chem. Soc.* **1979**, *101*, 445–449.

(4) Brown, J. N.; Teller, R. G. *J. Am. Chem. Soc.* **1976**, *98*, 7565–7569.

(5) Kessler, H.; Bats, J. W.; Griesinger, C.; Koll, S.; Will, M.; Wagner, K. *J. Am. Chem. Soc.* **1988**, *110*, 1033–1049.

(6) Kessler, H.; Klein, M.; Wagner, K. *Int. J. Pept. Protein Res.* **1988**, *31*, 481–498.